

Influence of Interfacial Delamination on Channel Cracking of Brittle Thin Films

Yaoyu Pang, and Rui Huang

Department of Aerospace Engineering and Engineering Mechanics, University of Texas at Austin, 1 University Station, C0600, Austin, TX, 78712

ABSTRACT

Channeling cracks in low-k dielectrics have been observed to be a key reliability issue for advanced interconnects. The constraint effect of surrounding materials including stacked buffer layers has been studied. This paper analyzes the effect of interfacial delamination on the fracture condition of brittle thin films on elastic substrates. It is found that stable delamination along with the growth of a channel crack is possible only for a specific range of elastic mismatch and interface toughness. An effective energy release rate is defined to account for the influence of interfacial delamination on both the driving force and the fracture resistance, which can be significantly higher than the case assuming no delamination.

INTRODUCTION

Integration of low-k and ultralow-k dielectrics in advanced interconnects has posed significant challenges for reliability issues resulting from compromised mechanical properties. Two common failure modes have been reported, one for cohesive fracture [1] and the other for interfacial delamination [2]. The former pertains to the brittleness of low-k materials subjected to tension, and the latter manifests for poor adhesion between low k and other materials [3]. This paper considers a possible failure mode with concomitant cohesive fracture and interfacial delamination.

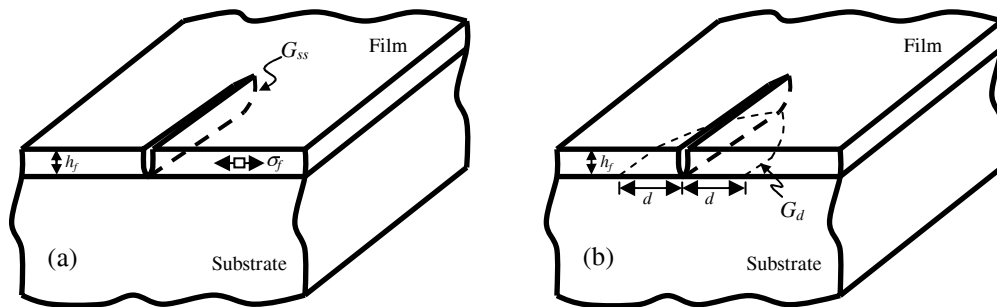


Fig. 1: (a) A channel crack with no interfacial delamination; (b) a channel crack with stable interfacial delamination of width d on both sides.

One common cohesive fracture mode for thin films under tension is channel cracking (Fig. 1). Previous studies have shown that the driving force for the steady state growth of a channel crack (i.e., energy release rate) depends on the constraint effect of surrounding layers [1,4]. For a brittle thin film on an elastic substrate, the driving force increases for increasingly compliant substrates [5,6]. The effect of constraint can be partly lost as the substrate deforms plastically [7] or creeps [8]. More recent studies have focused on the effects of stacked buffer layers [4,9] and patterned film structures [1]. In most of these studies, the interfaces between the film and the substrate or the buffer layers are assumed to remain perfectly bonded as the channel crack grows in the film (Fig. 1a). However, the stress concentration at the root of the channel crack may drive interfacial delamination [10]. While some experimental observations clearly

showed no delamination [4,11], others observed delamination of the interface at the root of channel cracks [4,12]. Two questions are yet to be answered: *Under what condition would the growth of a channel crack be accompanied by interfacial delamination (Fig. 1b) or otherwise? How would the interfacial delamination (if occurring) affect the driving force for fracture in thin film structures?* The present paper is our first attempt to answer these questions.

A CHANNEL CRACK WITHOUT DELAMINATION

As illustrated in Fig. 1a, assuming no interface delamination, the energy release rate for steady state growth of a channel crack in an elastic thin film bonded to an elastic substrate is

$$G_{ss} = Z(\alpha, \beta) \frac{\sigma_f^2 h_f}{\bar{E}_f}, \quad (1)$$

where σ_f is the residual tensile stress in the film, h_f is the film thickness, and \bar{E}_f is the plane strain modulus. The dimensionless coefficient Z depends on the elastic mismatch between the film and the substrate, through the Dundurs' parameters

$$\alpha = \frac{\bar{E}_f - \bar{E}_s}{\bar{E}_f + \bar{E}_s} \quad \text{and} \quad \beta = \frac{\bar{E}_f(1-\nu_f)(1-2\nu_s) - \bar{E}_s(1-\nu_s)(1-2\nu_f)}{2(1-\nu_f)(1-\nu_s)(\bar{E}_f + \bar{E}_s)}. \quad (2)$$

When the film and the substrate have identical elastic moduli, we have $\alpha = \beta = 0$ and $Z = 1.976$. The value of Z increases for a stiff film on a relatively compliant substrate ($\alpha > 0$) and decreases for a compliant film on a relatively stiff substrate ($\alpha < 0$) [5,6].

In general, the ERR can be calculated from a two-dimensional (2D) model [5,6], with

$$G_{ss} = \frac{\sigma_f}{2h_f} \int_0^{h_f} \delta(z) dz, \quad (3)$$

where $\delta(z)$ is the opening displacement of the crack surfaces in the 2D model.

INTERFACIAL DELAMINATION FROM CHANNEL ROOT

Consider an interface crack emanating from the channel root at each side (Fig. 1b). Far behind the channel front, the energy release rate (ERR) for the interface crack is

$$G_d = Z_d \left(\frac{d}{h_f}, \alpha, \beta \right) \frac{\sigma_f^2 h_f}{\bar{E}_f}, \quad (4)$$

where d is the width of delamination and Z_d is a dimensionless function that can be determined from a finite element model. When $d/h_f \rightarrow \infty$, the interface crack reaches the steady state with

$$G_{ss}^d = \frac{\sigma_f^2 h_f}{2\bar{E}_f}, \quad (5)$$

which is independent of the crack length as well as the elastic mismatch. The same problem was studied by Ye et al. [10], and two different edge effects on the interfacial delamination were analyzed by Yu et al. [13]. The steady state is the same for all edge conditions.

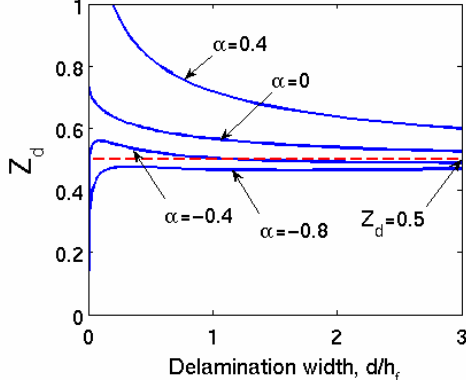


Fig. 2: Four types of behavior for interfacial delamination emanating from the root of a channel crack.

The interface toughness resisting delamination depends on the mode mix [14]. Typically, the phase angle for an interface crack quickly approaches a steady state

$$\psi_{ss} = \omega(\alpha, \beta), \quad (6)$$

as given in Ref. [14]. Due to the oscillatory singularity at the interface crack tip, a length scale has to be used to define the phase angle. Here we take the film thickness h_f as the length. When the film and the substrate have identical elastic moduli, $\psi_{ss} = \omega(0,0) = 52.1^\circ$. For convenience, in the subsequent discussions, we take the phase angle as a constant for each elastic mismatch.

Ye et al. [10] gave an approximate formula for Z_d with $\beta = \alpha/4$ ($\nu_f = \nu_s = 1/3$):

$$Z_d = \frac{1}{2} \left(\frac{d/h_f}{1 + d/h_f} \right)^{1-2s} \left[1 + \lambda_1 \exp \left(-\lambda_2 \sqrt{\frac{d}{h_f}} \right) \right], \quad (7)$$

where $s = s(\alpha, \beta)$ is the singularity parameter at the root of the channel crack, λ_1 and λ_2 are fitting parameters, as tabulated for various values of α in Ref. [10]. Figure 2 plots four types of interface behavior based on Eq. (7), discussed as follows.

- (i) When $\alpha > 0$ (a stiff film on a compliant substrate, $s > 0.5$), Z_d monotonically decreases from infinity and approaches the steady state. Two possible consequences exist: if the interface toughness $\Gamma_i(\psi_{ss}) < G_{ss}^d$, the interface crack will grow unstably, leading to spontaneous debonding; if $\Gamma_i(\psi_{ss}) > G_{ss}^d$, the interface crack arrests, resulting in a stable delamination with width d_s for which $\Gamma_i(\psi_{ss}) = G_{ss}^d(d_s)$.
- (ii) When $\alpha = 0$ (no elastic mismatch, $s = 0.5$), Z_d monotonically decreases from a finite value. As a result, there exists a maximum energy release, $G_{\max}^d = 1.496G_{ss}^d$. There are then three possible consequences: spontaneous debonding if $\Gamma_i(\psi_{ss}) < G_{ss}^d$, stable delamination if $G_{\max}^d > \Gamma_i(\psi_{ss}) > G_{ss}^d$, and no delamination if $\Gamma_i > G_{\max}^d$.

When $\alpha < 0$ (i.e., a compliant film on a stiff substrate, $s < 0.5$), Z_d necessarily starts from zero at $d/h_f = 0$. As d/h_f increases, Z_d first increases and then decreases, with a peak before it approaches the steady state. The peak ERR, G_{\max}^d , decreases as α decreases, and becomes less than G_{ss}^d for $\alpha < -0.6$. This renders two types of behavior for $\alpha < 0$:

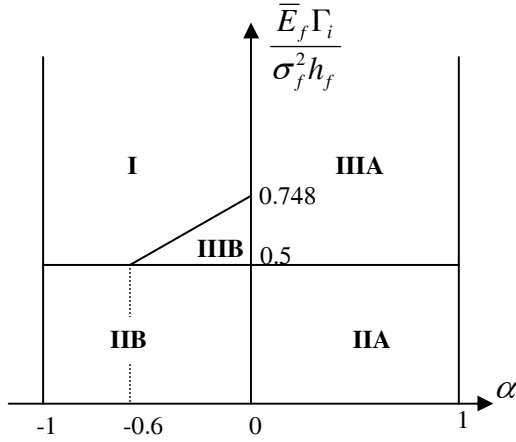


Fig. 3: A map for interfacial delamination from the root of a channel crack. (I) no delamination, (II) unstable spontaneous delamination, and (III) stable delamination, with barrierless initiation for IIA and IIIA while a critical defect size exists for IIB and IIIB.

- (iii) When $0 > \alpha > -0.6$, $G_{\max}^d > G_{ss}^d$. Similar to Case (ii), there are three possibilities. However, since the ERR now approaches zero for very short cracks, for both the spontaneous debonding and stable delamination, a critical initial defect size is required for the interface crack to grow, which sets a barrier for the initiation of delamination.
- (iv) When $\alpha < -0.6$, Z_d almost monotonically increases (with a very shallow peak below 0.5). There are thus only two possible consequences here: spontaneous debonding when $\Gamma_i(\psi_{ss}) < G_{ss}^d$ (with a barrier for initiation), or no delamination when $\Gamma_i(\psi_{ss}) > G_{ss}^d$.

Based on the above discussion, we construct a map for the different interface behavior in Fig. 3, for different combinations of elastic mismatch and interface toughness. Three regions are identified. Of particular interest to the present study is Region III, where a stable delamination can develop along with the channel crack. The stable delamination width, d_s , can then be determined as a function of the interface toughness, by setting $G_d = \Gamma_i(\psi_{ss})$, or in a dimensionless form

$$Z_d\left(\frac{d_s}{h_f}, \alpha, \beta\right) = \bar{\Gamma}_i = \frac{\bar{E}_f \Gamma_i(\psi_{ss})}{\sigma_f^2 h_f}. \quad (8)$$

A CHANNEL CRACK WITH STABLE DELAMINATION

With a stable delamination along each side of the channel crack (Fig. 1b), the substrate constraint on the opening of the channel crack is partly relaxed. The steady state ERR calculated from Eq. (3) becomes greater than Eq. (1). Dimensional consideration gives that

$$G_{ss}^* = Z^*\left(\frac{d_s}{h_f}, \alpha, \beta\right) \frac{\sigma_f^2 h_f}{\bar{E}_f}, \quad (9)$$

From an energetic consideration [10], we obtain that

$$G_{ss}^* = G_{ss} + \frac{2}{h_f} \int_0^{d_s} G_d(a) da, \quad (10)$$

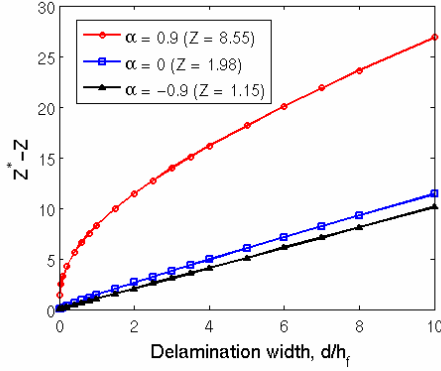


Fig. 4: Increase of the crack driving force due to interfacial delamination.

where $G_d(a)$ is the energy release rate for the interface crack of width a . When $d_s/h_f \rightarrow 0$, $Z^* \rightarrow Z$, recovering Eq. (1); when $d_s/h_f \rightarrow \infty$, $Z^* \rightarrow \infty$ (a freestanding film with an infinitely long crack). Furthermore, as $d_s/h_f \rightarrow \infty$, since the interface crack reaches the steady state, the change of the energy release rate is simply

$$\Delta G_{ss}^* = 2G_{ss}^d \frac{\Delta d}{h_f}, \text{ or } \Delta Z^* = \frac{\Delta d}{h_f}, \quad (11)$$

which dictates the limiting rate for the increase of ERR as the delamination width increases.

A finite element model is employed to calculate Z^* , which is plotted in Fig. 4 as a function of d/h_f for different elastic mismatch parameters. For a compliant film on a relative stiff substrate ($\alpha < 0$), the increase is almost linear for the entire range of delamination width. For a stiff film on a relatively compliant substrate ($\alpha > 0$), however, the increase is nonlinear for short interface delamination and then approaches a straight line of slope 1 as predicted by Eq. (11). Apparently, with interfacial delamination, the driving force for channel crack growth can be significantly higher as compared to the case assuming no delamination.

EFFECTIVE ENERGY RELEASE RATE

While the interfacial delamination relaxes the constraint on crack opening thus enhances the fracture driving force, it also requires additional energy to fracture the interface. If the increase in the energy release rate exceeds the energy needed for delamination, growth of the channel crack with the stable delamination is energetically favored. Otherwise, the channel crack with no delamination is favored. The competition can be understood from a unified fracture condition for both cases, namely

$$G_{ss}^* \geq \Gamma_f + W_d, \quad (12)$$

where Γ_f is the cohesive fracture toughness of the film, and W_d is the energy to delaminate the interface accompanying per unit area growth of the channel crack. Considering the delamination at both sides of the channel crack, the delamination energy is

$$W_d = \frac{2}{h_f} \int_0^{d_s} \Gamma_i(\psi(a)) da \approx 2\Gamma_i(\psi_{ss}) \frac{d_s}{h_f}. \quad (13)$$

When $d_s = 0$, Eq. (12) recovers the condition for cohesive fracture of the film.

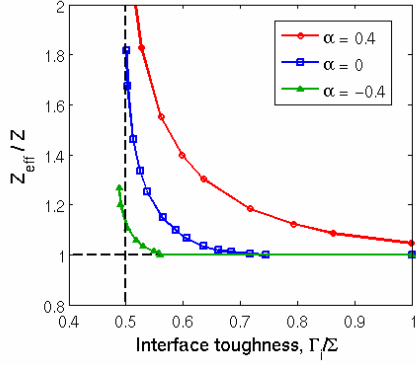


Fig. 5: Effective driving force for channel cracking as a function of the normalized interface toughness, $\bar{\Gamma}_i$.

Equation (12) may not be convenient to use directly, since both sides of the equation increases with interfacial delamination. By moving W_d to the left hand side, we define an effective driving force for growth of the channel crack with stable interfacial delamination:

$$G_{ss}^{eff} = G_{ss}^* - W_d = Z_{eff}(\bar{\Gamma}_i, \alpha, \beta) \frac{\sigma_f^2 h_f}{E_f}, \quad (14)$$

with

$$Z_{eff} = Z^* \left(\frac{d_s}{h_f}, \alpha, \beta \right) - 2\bar{\Gamma}_i \frac{d_s}{h_f}. \quad (15)$$

Figure 5 plots Z_{eff} as a function of $\bar{\Gamma}_i$ for different elastic mismatch parameters. For very strong interfacial adhesion ($\bar{\Gamma}_i \rightarrow \infty$), $d_s \rightarrow 0$ and $Z_{eff} \rightarrow Z$, which recovers the case for channel cracking with no delamination. For weak interfaces ($\bar{\Gamma}_i < 0.5$), spontaneous debonding is predicted. For an intermediate interface toughness, the channel crack grows with stable delamination, with a higher effective driving force ($Z_{eff} > Z$).

REFERENCES

1. X.H. Liu, M.W. Lane, T.M. Shaw, E.G. Liniger, R.R. Rosenberg, and D.C. Edelstein, Proc. Advanced Metallization Conference 2004, pp. 361-367.
2. X.H. Liu, M.W. Lane, T.M. Shaw, E. Simonyi, Int. J. Solids Struct. 44, 1706-1718 (2007).
3. T.Y. Tsui, A.J. McKerrow, and J.J. Vlassak, J. Mech. Phys. Solids 54, 887-903 (2006).
4. T.Y. Tsui, A.J. McKerrow, and J.J. Vlassak, J. Mater. Res. 20, 2266-2273 (2005).
5. J.L. Beuth, Int. J. Solids Struct. 29, 63-191 (1992).
6. R. Huang, J.H. Prevost, Z.Y. Huang, and Z. Suo, Eng. Frac. Mech. 70, 2513-2526 (2003).
7. J.M. Ambrico and M.R. Begley, Thin Solid Films 419, 144-153 (2002).
8. R. Huang, J.H. Prevost, and Z. Suo, Acta Mater. 50, 4137-4148 (2002).
9. N. Cordero, J. Yoon, and Z. Suo, Appl. Phys. Lett. 90, 111910 (2007).
10. T. Ye, Z. Suo, and A.G. Evans, Int. J. Solids Struct. 29, 2639-2648 (1992).
11. J. He, G. Xu, and Z. Suo, Proc. 7th Int. Workshop on Stress-Induced Phenomena in Metallization (Austin, Texas, 14-16 June 2004), pp. 3-14.
12. Z. Suo, Reliability of Interconnect Structures. In: *Interfacial and Nanoscale Fracture*, pp. 265-324 (Elsevier, Oxford, 2003).
13. H.H. Yu, M.Y. He, and J.W. Hutchinson, Acta Mater. 49, 93-107 (2001).
14. J.W. Hutchinson and Z. Suo, Advances in Applied Mechanics 29, 63-191 (1992).